Available online at www.sciencedirect.com
ScienceDirect
Polymer 47 (2006) 7846–7852
polymer
www.elsevier.com/locate/polymer

Computer simulation study on the shear-induced phase separation in semidilute polymer solutions in 3-dimensional space

Mikihito Takenaka [a,*], Shotaro Nishitsuji [a], Takashi Taniguchi [b], Masataka Yamaguchi [a], Koichiro Tada [a], Takeji Hashimoto [a]

[a] *Department of Polymer Chemistry, Graduate School of Engineering, Kyoto University, Kyoto-Daigaku-Katsura, Nishikyo-ku, Kyoto 615-8510, Japan*
[b] *Department of Polymer Science and Engineering, Yamagata University, Yonezawa 992-8510, Japan*

Received 20 March 2006; received in revised form 3 August 2006; accepted 7 August 2006
Available online 15 September 2006

Abstract

We investigated the shear-induced phase separation and/or concentration fluctuation phenomena in semidilute polymer solution by using computer simulation in 3-dimensional space with Doi–Onuki theory. The enhancement of the concentration fluctuations occurs under shear flow and the scattering function in q_x–q_z plane exhibits the so-called butterfly pattern as observed experimentally, where q_x and q_z are the components of the scattering vector for flow direction and neutral direction, respectively. The time changes in the peak position and the intensity at peak position in the scattering function in q_x–q_z plane can be divided into two regions: the peak position becomes smaller and the peak intensity increases with t, and then the peak position and intensity become constant and the system reaches its steady state. These agree with the experimental results qualitatively. However, the computer simulation results indicate that the peak position at the steady state is almost independent of the shear rate, while the decrease in the peak position at steady state with shear rate has been observed experimentally. This disagreement originates from the use of the simplest constitutive equation in the computer simulation.

Keywords: Shear-induced phase separation; Semidilute polymer solution; Doi–Onuki theory

1. Introduction

When shear flow is imposed to a semidilute polymer solution at its one phase region, the solution exhibits strong turbidity. This phenomenon is called shear-induced concentration fluctuation and/or phase separation and one of the remarkable properties of dynamically asymmetric binary systems where each component of the systems differs in the dynamical properties such as the self-diffusion coefficient and viscosity. In such systems, ''dynamical coupling between stress and diffusion'' [1] strongly affects the dynamics of the concentration fluctuations in the systems. The dynamical coupling arises from the spatial heterogeneity of the stress field associated with the thermal concentration fluctuations in the systems. The heterogeneity of the stress field influences the dynamics of the concentration fluctuations through the variation of the free energy function by the inhomogeneity. This coupling causes the following interesting phenomena as well as the shear-induced concentration fluctuations and/or phase separation of our interest in this work: nonexponential time correlation function of the concentration fluctuations was observed by dynamic light scattering in one phase region of the semidilute polymer solutions [2–5], the strong q^{-2} dependence of the Onsager kinetic coefficient due to the suppression of the diffusion by the coupling was found in the early-stage spinodal decomposition in the dynamically asymmetric systems [5–8], and a sponge-like network structure appears during the later-stage spinodal decomposition [9,10].

Experimentally, the shear-induced concentration fluctuations and/or phase separation of the semidilute solutions has

* Corresponding author. Tel.: +81 75 383 2622; fax: +81 75 383 2623.
E-mail address: takenaka@alloy.polym.kyoto-u.ac.jp (M. Takenaka).

0032-3861/$ - see front matter © 2006 Elsevier Ltd. All rights reserved.
doi:10.1016/j.polymer.2006.08.024

been observed mainly by light scattering (LS) [11–14] and small-angle neutron scattering (SANS) [14–17]. Saito and Hashimoto explored that there are two characteristic shear rates regarding the shear-induced structure formation observed in the q_x–q_z plane as a function of $\dot{\gamma}$ [18]. Here $\mathbf{q}$ is the scattering wave vector and the magnitude q of $\mathbf{q}$ is defined as $q = (4\pi/\lambda)\sin(\theta/2)$ with λ and θ being the wavelength of the incident beam and the scattering angle in the medium, respectively. The coordinates x, y, and z indicate, respectively, the flow direction, the velocity gradient direction and neutral direction and q_x, q_y, and q_z are the respective components of $\mathbf{q}$. One is $\dot{\gamma}_{cx}$ at which the LS intensity along the flow direction (q_x) starts to increase in the q_x–q_z plane. At higher $\dot{\gamma}$ than $\dot{\gamma}_{cx}$, the unique scattering so-called ''butterfly pattern'', a pair of symmetric wings along q_x direction, appeared in the q_x–q_z plane. Another is $\dot{\gamma}_{cz}$, at which the LS intensity along q_z starts to increase [15,17]. $\dot{\gamma}_{cz}$ is believed to be a shear rate from which the shear-induced instability starts to occur. In our previous studies [18,19], we have elucidated the temperature and concentration dependences of $\dot{\gamma}_{cx}$ for a given solvent and the solvent quality dependence of $\dot{\gamma}_{cx}$. Wu et al. found an increase in the scattered intensity in the q_x–q_z plane with LS [11] under shear field. In the q_x–q_z plane, the scattered intensity was enhanced in the first and third quadrants of q_x–q_z plane.

Theoretically, Helfand and Fredrickson [20], Milner [21], and Onuki [22] (HFMO) have developed the dynamical equation of the concentration fluctuations. The equation includes the gradient term of the stress tensor as well as Ginzburg–Landau type free energy functional to account for the stress–diffusion coupling. Milner [21], and Ji and Helfand [23] calculated the structure factor by using linearized HFMO theory, and found the increase in structure factors under shear flow. We also calculated the structure factor by using the linearized theory with the Kaye–BKZ constitutive equation to express the non-Newtonian behavior and the normal stress effect [24] and found the butterfly pattern in the q_x–q_z plane which is observed experimentally above the critical shear rate.

The computer simulation including the nonlinear term of HFMO theory has been done by Onuki et al. [25] and Okuzono [26]. Onuki et al. have numerically integrated HFMO theory while Okuzono used the smoothed particle hydrodynamics method to investigate shear-induced phase separation. They observed that the shear-induced phase separation occurs under shear flow in their simulations. However, they did computer simulation in 2-dimensional space and observed the concentration fluctuation field and the structure factor in the x (flow direction)–y (velocity gradient direction) plane. On the other hand, we observed the shear-induced concentration fluctuations and/or phase-separation phenomena by using scattering techniques in q_x–q_z plane, in real experiments. The unique butterfly scattering pattern is observed in this q_x–q_z space in real experiments. The computer simulations in 2-dimensional space are, thus, not sufficient to compare the results of the simulation of the real experiments. Therefore, in this study, in order to enable us to compare between them, we shall present the computer simulation based on a time-dependent Ginzburg–Landau type equation proposed by HFMO in 3-dimensional space. In Section 2, we will present the dynamical equation including the stress–diffusion coupling and the reduced equations used in the simulation. In Section 3, we will show the simulation results in real and reciprocal spaces under various shear rates. Finally we will conclude our results in Section 4.

2. Simulation scheme

In this section, we will present a dynamic model of a semi-dilute polymer solution in which the polymer volume fraction ϕ satisfies $\phi > \phi_c$ and $\phi \ll 1$ with $\phi_c = N^{-1/2}$ and N being, respectively, the critical volume fraction of the system and the polymerization index [27]. We introduce a tensor variable $\overleftrightarrow{\mathbf{W}}$, called the conformation tensor, to represent chain deformations. In terms of ϕ and $\overleftrightarrow{\mathbf{W}}$, the free energy is given by [21,22,25,28]

$$F\{\phi,\overleftrightarrow{\mathbf{W}}\} = \int \mathrm{d}\mathbf{r}\left[f(\phi) + \frac{1}{2}C(\phi)|\nabla\phi|^2 + \frac{1}{4}G(\phi)\sum_{ij}\left(W_{ij}-\delta_{ij}\right)^2\right] \tag{1}$$

Here

$$f(\phi) \cong \left(\frac{k_B T}{v_0}\right)\left[\frac{\phi\ln\phi}{N} + \left(\frac{1}{2}-\chi\right)\phi^2 + \frac{1}{6}\phi^3\right] \tag{2}$$

is the Flory–Huggins free energy density where v_0 and χ are, respectively, the volume of a monomer and the Flory–Huggins interaction parameter per monomer [27]. In the second term, $C(\phi)$ is proportional to ϕ^{-1} from scaling theory. The last term expresses the elastic energy of the entangled polymer network with $G(\phi)$ being the plateau modulus of the entangled polymer network at ϕ. The ϕ-dependence $G(\phi)$ is given by

$$G(\phi) = G_0\frac{k_B T}{v_0}\phi^3, \tag{3}$$

where G_0 is the plateau modulus at bulk state. For simplicity we assume that the deviation of $\overleftrightarrow{\mathbf{W}}$ from the equilibrium value $\overleftrightarrow{\mathbf{I}}$ (= unit tensor) is so small that the elastic free energy is bilinear in $\overleftrightarrow{\mathbf{W}} - \overleftrightarrow{\mathbf{I}}$. Since the motion of $\overleftrightarrow{\mathbf{W}}$ is determined by the polymer velocity $\mathbf{v}_p$ its simplest dynamics equation is given by [22,28,29]

$$\frac{\partial}{\partial t}\overleftrightarrow{\mathbf{W}} + \left(\mathbf{v}_p\cdot\nabla\right)\overleftrightarrow{\mathbf{W}} = \overleftrightarrow{\mathbf{D}}\cdot\overleftrightarrow{\mathbf{W}} + \overleftrightarrow{\mathbf{W}}\cdot\overleftrightarrow{\mathbf{D}}^{\mathrm{T}} - \frac{1}{\tau(\phi)}\left(\overleftrightarrow{\mathbf{W}} - \overleftrightarrow{\mathbf{I}}\right) \tag{4}$$

where $D_{ij} = \partial v_{pi}/\partial x_j$ is the gradient tensor of $\mathbf{v}_p$ and $\overleftrightarrow{\mathbf{D}}^{\mathrm{T}}$ is the transposed tensor of $\overleftrightarrow{\mathbf{D}}$. The relaxation time $\tau(\phi)$ corresponds to the longest relaxation time of the solution at ϕ and its ϕ-dependence is given by

$$\tau = \tau_0\phi^3, \tag{5}$$

where τ_0 is the longest relaxation time at bulk state. From Eqs. (1) and (4) we may calculate free energy changes against infinitesimal motion of the network to obtain the network stress

$$\boldsymbol{\sigma}_{\mathrm{p}} = 2\overleftrightarrow{\mathbf{W}}\frac{\delta F}{\delta \overleftrightarrow{\mathbf{W}}} = G(\phi)\,\overleftrightarrow{\mathbf{W}}\cdot(\overleftrightarrow{\mathbf{W}} - \overleftrightarrow{\mathbf{I}}). \tag{6}$$

In the case when the deformation rate of the polymer or the shear rate $\dot{\gamma}$ is much slower than τ^{-1}, we have $W_{ij} - \delta_{ij} \cong \tau(D_{ij} + D_{ji})$ and obtain the Newtonian viscosity $\eta_{\mathrm{p}} = G(\phi)\tau(\phi)$ which is supposed to be much larger than the solvent viscosity η_0 in the semidilute case. On the other hand, in the case when the deformation rate of polymer or the shear rate $\dot{\gamma}$ is much faster than τ^{-1}, the solution behaves as a gel and $W_{ij} - \delta_{ij} \cong (\partial u_{\mathrm{p}i}/\partial x_j + \partial u_{\mathrm{p}j}/\partial x_i)$, where $\boldsymbol{u}_{\mathrm{p}}$ is the time integral of $\mathbf{v}_{\mathrm{p}}$ and the displacement of the network.

The solvent velocity $\mathbf{v}_{\mathrm{s}}$ and the polymer velocity $\mathbf{v}_{\mathrm{p}}$ are different when the diffusion is taking place. The volume fraction is convected by $\mathbf{v}_{\mathrm{p}}$ as

$$\frac{\partial}{\partial t}\phi = -\nabla\cdot\left(\phi\mathbf{v}_{\mathrm{p}}\right). \tag{7}$$

For slow motions we may neglect the acceleration of the average velocity $\mathbf{v} = \phi\mathbf{v}_{\mathrm{p}} + (1-\phi)\mathbf{v}_{\mathrm{s}}$ to obtain

$$\eta_0\nabla^2 v = \nabla\cdot\left[C(\nabla\phi)(\nabla\phi) - \overleftrightarrow{\boldsymbol{\sigma}}_{\mathrm{p}}\right]_{\perp} \tag{8}$$

where $[\cdots]_{\perp}$ denotes taking the transverse part. For simplicity we assume that the mass densities of the pure polymer and solvent are the same and that the fluid is incompressible, so $\nabla\cdot\mathbf{v} = 0$ holds. Furthermore, on the assumption that the network stress acts on the polymer and not directly on the solvent [1], a two fluid model gives the relative velocity $\mathbf{w} = \mathbf{v}_{\mathrm{p}} - \mathbf{v}_{\mathrm{s}}$ as

$$\zeta(\phi)\mathbf{w} = -\phi\nabla\frac{\delta F}{\delta\phi} + \nabla\cdot\overleftrightarrow{\boldsymbol{\sigma}}_{\mathrm{p}} + \frac{1}{4}G(\phi)\nabla\sum_{ij}\left(W_{ij} - \delta_{ij}\right)^2, \tag{9}$$

where $\zeta(\phi)$ is the friction coefficient and is given by

$$\zeta(\phi) = 6\pi\eta_0 a^{-2}\phi^2 \tag{10}$$

with a being the statistical segment length of the polymer. The last two terms in Eq. (9) show how diffusion is influenced by viscoelasticity. We numerically integrate Eqs. (4) and (7) on a $64\times64\times64$ cubic lattice as shown in Fig. 1. We employed the periodic boundary condition for x and z axes and Lees–Edwards boundary condition for y axis. Note that $\mathbf{v}$ and $\mathbf{w}$ have been expressed in terms of ϕ and $\mathbf{W}_{ij}$. We used the reduced variables for space, time and volume fraction with the units of the correlation length of the concentration fluctuations ξ defined by

$$\xi = R_{\mathrm{g}}\left[2\phi_0\{\phi_0 + \phi_0^{-1} - 2(\chi - \chi_{\mathrm{S}})\}\right]^{-1/2}, \tag{11}$$

the characteristic time t_0 defined by

$$t_0 = \frac{\xi^2}{\sqrt{6}D\left\{\phi_0 + \phi_0^{-1} - 2(\chi - \chi_{\mathrm{S}})\right\}}, \tag{12}$$

and the critical volume fraction ϕ_{c}, where R_{g}, ϕ_0, χ, χ_{S}, and D are, respectively, the radius of gyration of the polymer, the space-averaged $\phi(\mathbf{r})$, Flory–Huggins interaction parameter, Flory–Huggins interaction parameter at spinodal point, and the translational diffusion coefficient of the polymer. In order to use the similar condition with previous experiments [18], we set $N = 5.25\times10^4$, $\phi_0 = 6.4$, $\phi_{\mathrm{c}} = 6.4N^{-1/2}$, the reduced longest relaxation time at ϕ_0 $\tilde{\tau} = \tau_0\phi_0^3/t_0 = 10$, the reduced plateau modulus at bulk state $\tilde{G}_0 = 10$, and $\delta\tilde{\chi} = N^{1/2}(\chi - \chi_{\mathrm{S}}) = 0.6$, where $\tilde{G}_0$ is defined by

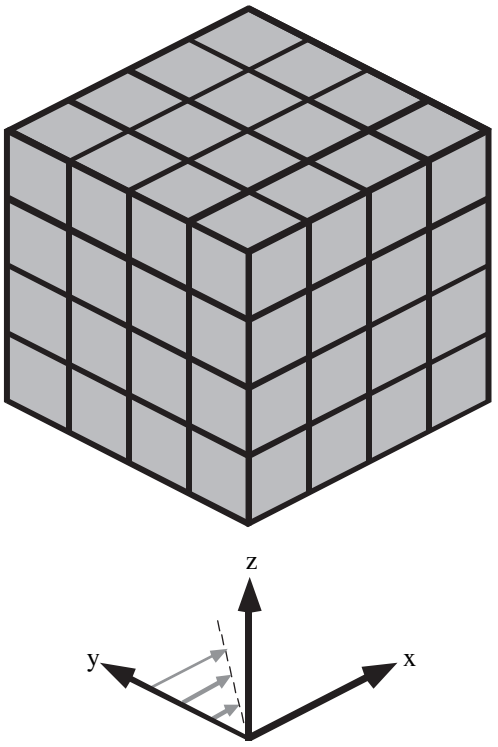

Fig. 1. Coordinates of the computer simulation in 3-dimensional space. x, y, and z axes correspond to velocity, velocity gradient, and neutral directions, respectively.

$$\tilde{G}_0 = \frac{G_0 v_0}{k_{\mathrm{B}}T\phi_0^2 N^{1/2}\left(\tilde{\phi}_0 + \tilde{\phi}_0^{-1} - 2\delta\tilde{\chi}\right)} \tag{13}$$

with $\tilde{\phi}_0 = \phi_0/\phi_{\mathrm{c}}$. The grid size is $\Delta\tilde{r} = \Delta r/\xi = 1$ and the time step is $\Delta\tilde{t} = \Delta t/t_0 = 1.0\times10^{-3}$. In the initial state at the reduced time $\tilde{t} = t/t = 0$, $\phi(\mathbf{r})$ at each lattice point is given by a Gaussian random number with $\langle[(\phi(\mathbf{r}) - \phi_0)/\phi_0]^2\rangle = 0.01$.

3. Results and discussion

Fig. 2 shows the time change in the concentration fluctuations in 3-dimensional space under no shear flow (a) and shear flow with reduced shear rate $\dot{\gamma}t_0 = 0.05$ (b). In the case of the simulation without shear flow, the initial concentration disappears in the field and its distribution becomes narrower with time. It is expected that the distribution becomes zero at long time limit since the effects of thermal noise are neglected in this simulation. On the other hand, in the case of the simulation under the shear flow with $\dot{\gamma}t_0 = 0.05$, the concentration

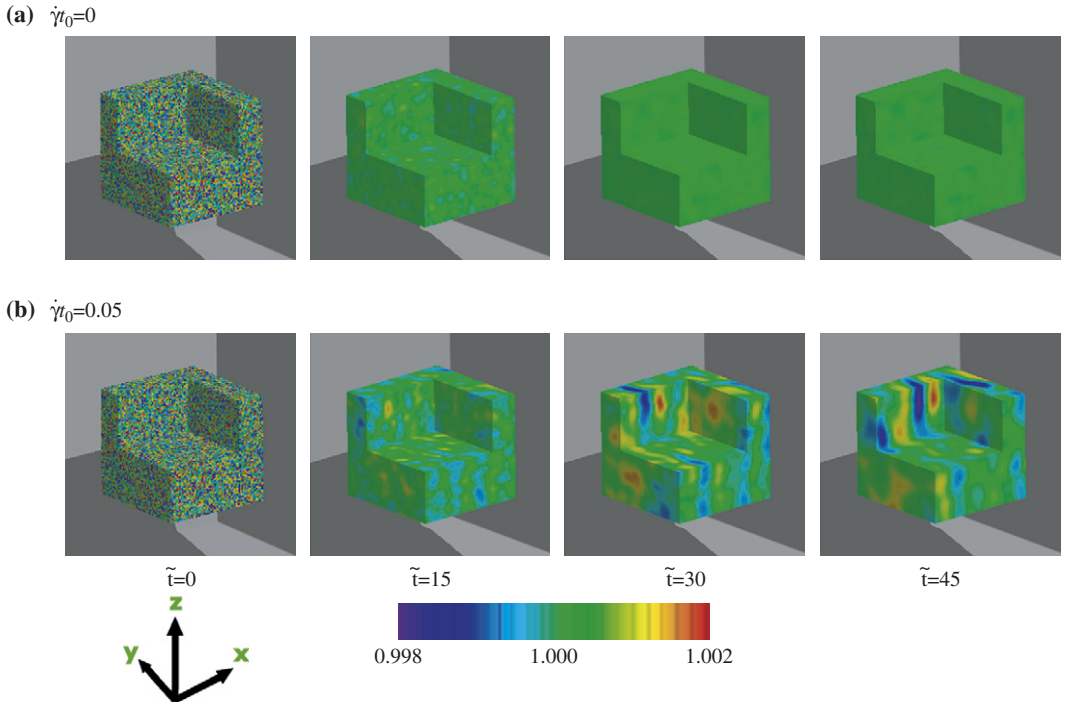

Fig. 2. Time changes in the concentration fluctuations in 3-dimensional space at (a) $\dot{\gamma}t_0 = 0$ and (b) $\dot{\gamma}t_0 = 0.05$. The coordinate direction is defined in the figure. x, y, and z axes correspond to velocity, velocity gradient, and neutral directions, respectively.

fluctuations appear and coarsen with time, indicating that the shear-induced phase separation occurs under shear flow.

Let us focus on the time changes in the scattering functions and the corresponding cross-sections of real space images of the concentration fluctuations. In the case of the simulation without shear flow, we did not observe the decay in the scattered intensity in q_x–q_y and q_x–q_z planes although we do not show the results of the simulation without shear flow here. The corresponding cross-sections of real space images in x–y and x–z planes also do not have any correlated fluctuations.

On the other hand, as shown in Fig. 3, the increase in the scattering function in both planes is observed under the shear flow with $\dot{\gamma}t_0 = 0.05$. In q_x–q_y plane, which corresponds to that usually observed by light scattering experiment, the scattered intensity increases along $q_z = 0$ with time and the peaks along $q_z = 0$ appear and shift towards smaller q with time. The scattering distribution at $\tilde{t} = 45$ exhibits so-called "butterfly pattern" which is a unique one observed in the shear-induced phase-separation phenomena. The time change in the scattering pattern is qualitatively in agreement with those in experimental results of semidilute PS/DOP solutions. The time changes in the cross-sections of real space images of x–z plane also show that the wavelength and amplitude of the concentration fluctuations grow with time. The orientation of concentration fluctuations aligned perpendicular to the shear flow at $\tilde{t} = 45$, which agrees with the structure factors. In q_y–q_z plane, the similar peaks develop and shift towards smaller q along $q_y = 0$. The enhancement of the structure factors is observed in the first and third quadrants of q_x–q_z plane, agreeing with the experimental results [11]. The corresponding cross-sections of the real space images of x–y plane also exhibit the tilted domain structures. This tilting is caused by the effects of the shear stress discussed previously [24].

Fig. 4 shows the changes in the peak position, q_m, of the scattering patterns and peak intensity, I_m, with time. The time changes can be classified into two regions. In earlier time region $\tilde{t} < 60$, q_m decreases while I_m increases with time. Although the variation of q_m and I_m with time is small, we fitted the time changes in q_m and I_m with the following power laws to characterize the tendency of the time changes:

$$q_m \sim \tilde{t}^{-\alpha},\ I_m \sim \tilde{t}^{\beta}, \tag{14}$$

and evaluated $\alpha = 0.23$ $(20 < \tilde{t} < 60)$ and $\beta = 3.7$ $(20 < \tilde{t} < 50)$ for $\dot{\gamma}t_0 = 0.05$. These time changes are due to the evolution of both amplitude and wavelength of the concentration fluctuations with time. In the later time region, $\tilde{t} > 60$, q_m and I_m become almost independent of time since the system has reached the steady state under shear flow. This behavior agrees with the experimental result qualitatively. However, the power laws of q_m and I_m to $\tilde{t}$ are different from those obtained from the experiment by Kume et al. [30] ($\alpha = 1.11$ and $\beta = 4.65$). This is due to the fact that we used the constitutive equation expressed by Eq. (4) although we have to use the theory which can be well expressed by the viscoelastic behavior of polymer solution such as Mead–Larson–Doi constitutive equation [31].

Fig. 5 shows the shear rate dependence of the structure factors in q_x–q_z plane and the corresponding cross-section images in x–z plane. The structure factors are enhanced and the wings of butterfly patterns are spread more widely along q_z

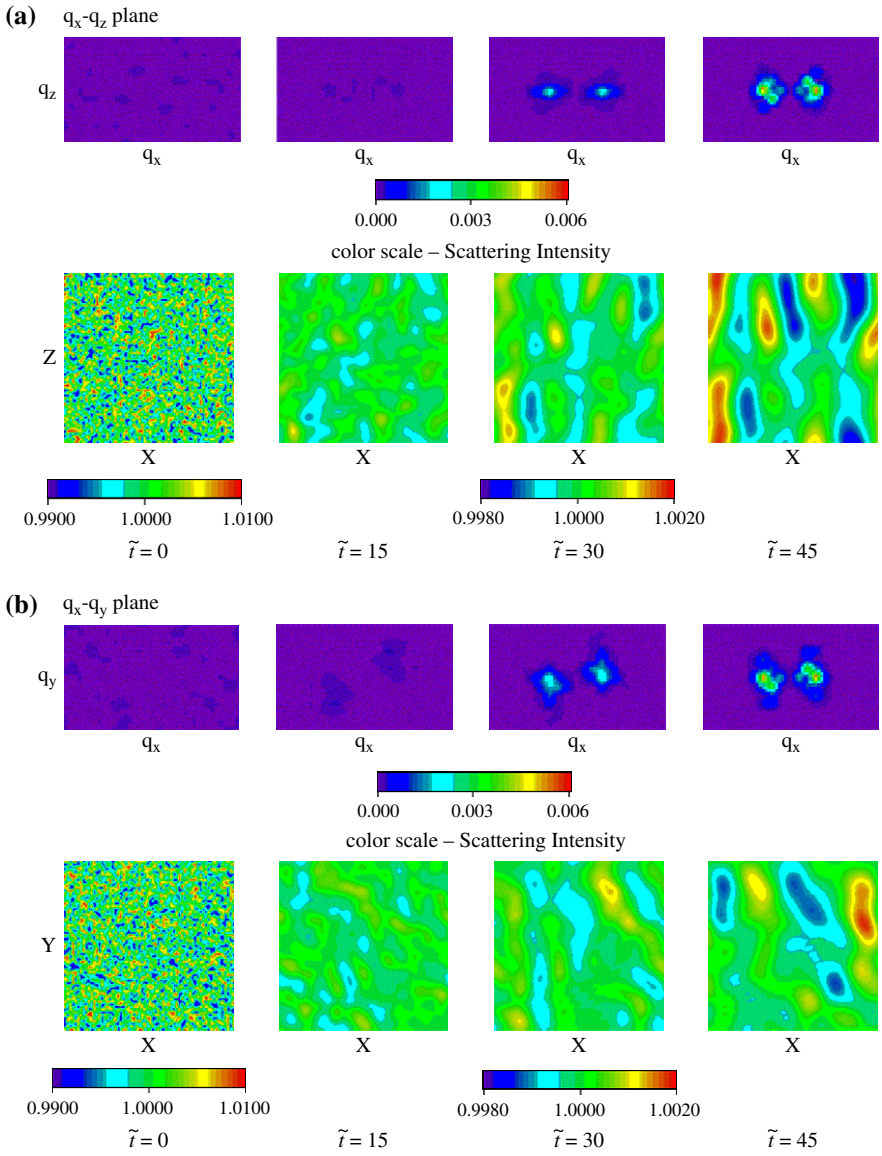

Fig. 3. Time changes in (a) the 2-dimensional structure factors in q_x–q_z plane and the cross-sections of the concentration fluctuations at $y = 32$ in x–z plane, and (b) the 2-dimensional structure factors in q_x–q_y plane and the cross-section of the concentration fluctuations at $z = 32$ in x–y plane at $\dot{\gamma}t_0 = 0.05$.

direction with $\dot{\gamma}$, which agree with the experimental results. The peak intensity I_m at steady state increases with $\dot{\gamma}$ while the peak position of the scattered intensity $q_{mc,z}$ along q_z axis at steady state seems to be independent of $\dot{\gamma}$. As for the cross-section, the amplitude of the concentration fluctuations increases with $\dot{\gamma}$, which coincides with the $\dot{\gamma}$ dependence of the structure factors. Fig. 6 shows the shear rate dependence of $q_{mc,z}$. $q_{mc,z}$ is almost independent of $\dot{\gamma}$, which does not agree with the experimental results where $q_{mc,z}$ decreases with $\dot{\gamma}$. Saito et al. reported that the increase in $q_{mc,z}$ with $\dot{\gamma}$ was found as the result of the calculation of the linearized theory of Doi–Onuki theory including BKZ-type constitutive equation for viscoelasticity contrary to the experimental results [24]. As suggested by Saito et al., this disagreement is due to the fact that the nonlinear term in thermodynamic term is neglected in the calculation [24]. However, even though our simulation includes the nonlinear term, the results have not agreed with the experimental results. This is also due to the fact that we used the simplest constitutive equation.

In the case of a semidilute polymer system subjected to shear flow, the longest relaxation time τ_m characterizes the critical condition of the shear-induced concentration fluctuations and/or phase separation. When the shear rate $\dot{\gamma}$ is smaller than the inverse of the longest relaxation time τ_m^{-1} of the solution, the local stress originating from the chain stretching is relaxed via disentanglement processes or usual translational diffusion processes of entangled polymers and the stress field through the free energy functional does not affect the dynamics of the concentration fluctuations, and hence no enhancement of the concentration fluctuations is expected under this situation. However, when $\dot{\gamma}$ is larger than τ_m^{-1}, the local stress cannot be relaxed by disentanglement. Instead, the squeeze of

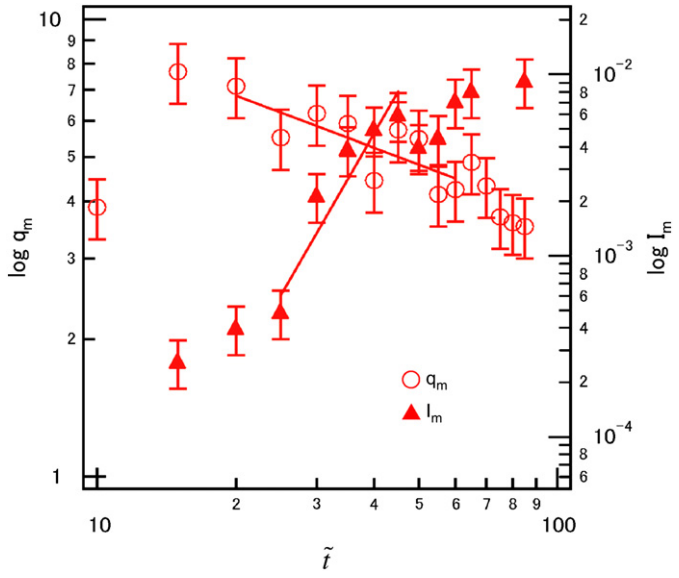

Fig. 4. Peak position q_m (open circle) and peak intensity I_m (filled triangle) of the structure factors are plotted as a function of $\tilde{t}$ at $\dot{\gamma}t_0 = 0.05$. The solid lines indicate the fitting results with the power laws expressed by Eq. (14).

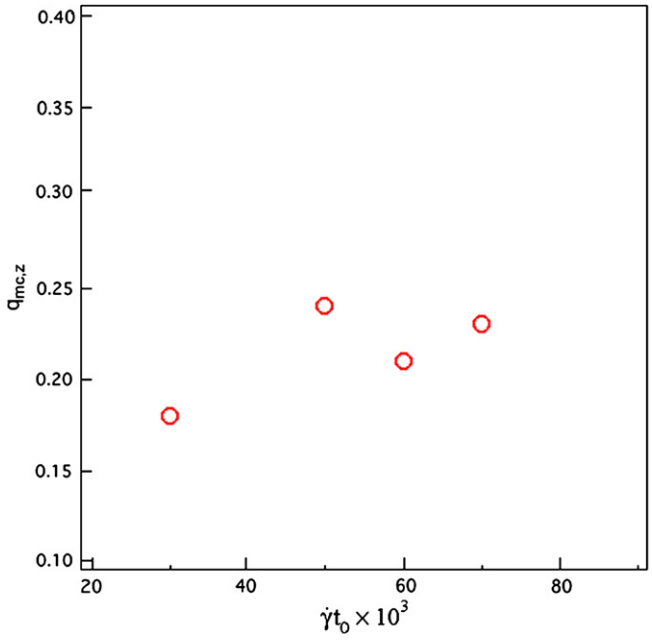

Fig. 6. $q_{mc,z}$ at steady state is plotted as a function of $\dot{\gamma}t_0$.

solvents to relax the stretching chains occurs in the regions having more entanglement points and hence larger stress. This process accompanies a further enhancement of concentration fluctuations. As $\dot{\gamma}$ is increased further, the shear-induced phase separation is eventually brought about. The global motions of this solvent squeezing are expressed by the longest relaxation process of polymer chains. However, local motions of the solvent squeezing such as the retraction of polymer chains are governed by collective motions of entangled polymer chains. These collective motions are not expressed in the constitutive equations used in this study. Thus the collective motions do not reflect the free energy functional of the system in this simulation so that the simulation results cannot describe the experimental results quantitatively.

4. Summary

We investigated the shear-induced phase separation and/or concentration fluctuation phenomena in semidilute polymer solution by using computer simulation in 3-dimensional space with Doi–Onuki theory. The enhancement of the concentration fluctuations occurs under shear flow and the so-called butterfly pattern appears in q_x–q_z plane as experimentally observed. The time changes in the peak position and the intensity at the peak position of the structure factors can be divided into two regions: the peak position becomes smaller and the peak intensity increases with t, and then the peak position and intensity become constant, which agrees with the experimental results. However, the peak position at steady state is independent

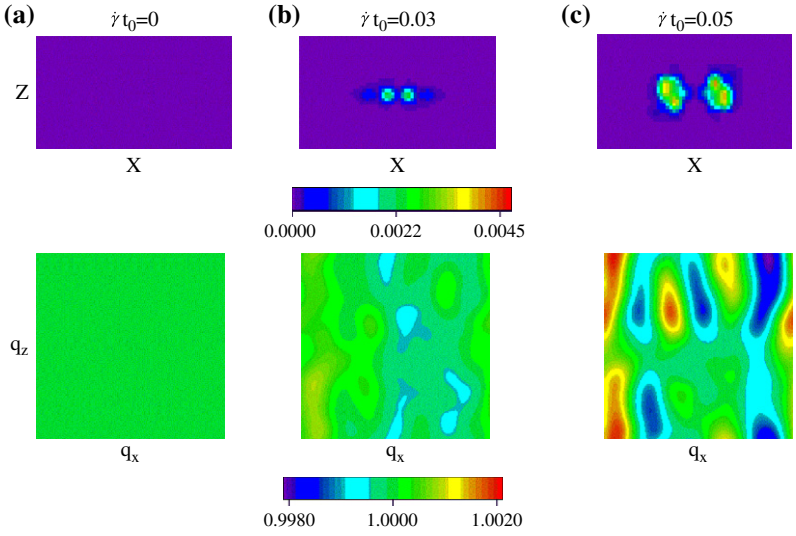

Fig. 5. Structure factors in q_x–q_z plane and the cross-sections of the concentration fluctuations at $y = 32$ in x–z plane in steady state ($\tilde{t} = 50$) at (a) 0.01, (b) 0.05 and (c) 0.06 $\dot{\gamma}t_0$.

of shear rate, although the decrease in the peak position with shear rate has been observed experimentally. This is because we employed the simplest constitutive equation which cannot describe the local motions of polymer chains. In order to compare the experiments with the computer simulation, we need to use the constitutive equation which can describe the rheology of the semidilute polymer solutions more quantitatively, such as Mead–Larson–Doi constitutive equation [31]. This will be the future work.

References

[1] Doi M, Onuki A. J Phys II (France) 1992;2:1631.
[2] Dixon PK, Pine DJ, Wu X-L. Phys Rev Lett 1992;68:2239.
[3] Fujita H. Studies in polymer science, vol. 9. Amsterdam: Elsevier; 1990.
[4] Einaga Y, Karube D. Polymer 1998;40:157.
[5] Toyoda N, Takenaka M, Saito S, Hashimoto T. Polymer 2001;42: 9193.
[6] Takenaka M, Takeno H, Hasegawa H, Saito S, Hashimoto T, Nagao M. Phys Rev E 2002;65:021806.
[7] Takenaka M, Takeno H, Hashimoto T, Nagao M. J Appl Crystallogr 2003;36:642.
[8] Schwahn D, Janssen S, Springer T. J Chem Phys 1992;97:8775.
[9] Tanaka H. Phys Rev Lett 1996;76:787.
[10] Tanaka H. Phys Rev Lett 1993;71:3158.
[11] Wu X-L, Pine DJ, Dixon PK. Phys Rev Lett 1991;66:2408.
[12] Hashimoto T, Fujioka K. J Phys Soc Jpn 1991;60:356.
[13] Hashimoto T, Kume T. J Phys Soc Jpn 1992;61:1839.
[14] Saito S, Matsuzaka K, Hashimoto T. Macromolecules 1999;32:4879.
[15] Morfin I, Lindner P, Boue F. Macromolecules 1999;32:7208.
[16] Boue F, Lindner P. Europhys Lett 1994;25:421.
[17] Saito S, Hashimoto T, Morfin I, Lindner P, Boue F. Macromolecules 2002;35:445.
[18] Saito S, Hashimoto T. J Chem Phys 2001;114:10531.
[19] Endoh MK, Saito S, Hashimoto T. Macromolecules 2002;35:7692.
[20] Helfand E, Fredrickson GH. Phys Rev Lett 1989;62:2468.
[21] Milner ST. Phys Rev E 1993;48:3674.
[22] Onuki A. Phys Rev Lett 1989;62:2472.
[23] Ji H, Helfand E. Macromolecules 1995;28:3869.
[24] Saito S, Takenaka A, Toyoda N, Hashimoto T. Macromolecules 2001; 34:6461.
[25] Onuki A, Yamamoto R, Taniguchi T. J Phys II (France) 1997;7:295.
[26] Okuzono T. Mod Phys Lett B 1997;11:379.
[27] de Gennes PG. Scaling concepts in polymer physics. Ithaca: Cornell University; 1979.
[28] Onuki A. J Phys Soc Jpn 1990;59:3423.
[29] Bird RB, Armstrong RC, Hassager O. Dynamics of polymeric liquids. New York: John Wiley; 1977.
[30] Kume T, Hattori T, Hashimoto T. Macromolecules 1997;30:427.
[31] Mead DW, Larson RG, Doi M. Macromolecules 1998;31:7895.